

Supporting Information

“Anti-electrostatic” halogen bonding in solution

Cody Loy,^a Jana M. Holthoff,^b Robert Weiss,^c Stefan M. Huber,^{*b} and Sergiy V. Rosokha^{*a}

Table of Content	Pages
Details of UV-Vis measurements and calculations of the equilibria constants	S2
Figure S1. Dependence of Δ Abs on concentration of I ⁻ for the solutions of 1 in CH ₃ CN	S4
Figure S2. UV-Vis spectra of mixtures of iodide with TDACl (A) or 2TDA (B) in CH ₃ CN	S4
Figure S3. Dependence of NMR shift of proton of 2 on concentration of I ⁻ in CD ₃ CN	S5
Figure S4. Dependence of UV-Vis spectra and Δ Abs on concentration of I ⁻ for the solutions of 1 in CH ₂ Cl ₂	S5
Figure S5. Dependence of UV-Vis spectra and Δ Abs on concentration of Br ⁻ for the solutions of 1 in CH ₃ CN	S6
Figure S6. Dependence of UV-Vis spectra and Δ Abs on concentration of Cl ⁻ for the solutions of 1 in CH ₃ CN	S6
Figure S7. Optimized geometries, AIM and NCI analysis of the AEXB [1 , Br ⁻] and [1 , Cl ⁻] complexes	S7
Table S1. Characteristics of the (3,-1) bond critical points along I ⁻ ⋯X ⁻ halogen bonds in the AEXB [1 , X ⁻] complexes.	S7
Figure S8. MO shapes and energies, and electronic transitions in the AEXB [1 , X ⁻] complexes	S7
Table S2. Energies and HOMO/LUMO energies of the calculated AEXB [1 , X ⁻] complexes	S8
Table S3. Calculated characteristics of the hypothetical anion- π [1 , X ⁻] complexes.	S9
Atomic coordinates of the optimized AEXB complexes	S9

^a Department of Chemistry
Ball State University
Muncie, Indiana 47306 USA
E-mail: svrosokha@bsu.edu

^b Fakultät für Chemie und Biochemie
Ruhr-Universität Bochum
Universitätsstr. 150, 44801 Bochum, Germany
E-mail: stefan.m.huber@rub.de

^c Institut für Organische Chemie
Friedrich-Alexander-Universität Erlangen-Nürnberg
Henkestr. 42, 91054 Erlangen, Germany

Details of the UV-Vis measurements and evaluation of equilibrium constant K.

Formation constants (K), of the XB complexes [**1**, X⁻] between 1,2-bis(dicyanomethylene)-3-iodo-cyclopropanide anion (**1**) (taken as salt with tris(dimethylamino)cyclopropenium counter-ions) and halide anions (X = Cl, Br, I) were established via UV-Vis measurements of the acetonitrile or dichloromethane solutions containing mixtures of these reactants. The measurements were carried out under argon atmosphere (in a Teflon-capped 1 mm-cuvette equipped with a sidearm) on a CARY 500 spectrophotometer at 22 °C. For each [**1**, X⁻] complex, the values of K were established based on the UV-Vis measurements of 3 - 5 series of solutions. Each series included 10 - 18 solutions. The concentrations of **1** (about 1 mM) were kept constant in each series and the concentrations of halides varied from 0 to 0.25 M. (Halides were taken as salts with tetra-*n*-butyl- or tetra-*n*-propylammonium cations, Bu₄NX or Pr₄NX, measurements with both cations afforded the same - within accuracy limit - formation constants). The ionic strength of the solutions was kept constant with Bu₄NPF₆.

In a typical series of measurements, stock solutions of individual **1** (10.0 mL, ~2.0 mM), Bu₄NX (5.00 mL, 0.50 M) and Bu₄NPF₆ (5.00 mL, 0.50 M) in CH₃CN (or CH₂Cl₂) were prepared in Schlenk tubes under Ar atmosphere. (The solvents were freshly distilled over P₂O₅ under argon.) Then, 0.500 mL of the solution of **1** were mixed in Teflon-capped (1 mm) cuvettes with x mL of stock solution of Bu₄NX and (0.500-x) mL of 0.50 M solution of Bu₄NPF₆ (where x typically were 0.500, 0.400, 0.330, 0.250, 0.200, 0.160, 0.130, 0.100, 0.080, 0.065, 0.050, 0.035, 0.020 or similar numbers) using gas-tight micro syringes with capacities from 0.050 mL to 0.500 mL. The UV-vis spectra were measured immediately after mixing. (Control experiments taken 5 – 20 min after mixing showed no substantial changes of absorption of the solutions containing **1** and I⁻ or Br⁻ anions. However, small spectral changes were observed in solutions with Cl⁻ anions if measurements were repeated 10 – 20 min after mixing.) Alternatively, series of UV-Vis measurements with I⁻ or Br⁻ anions were done by mixing 0.250 mL of the stock solution of **1** (prepared as described above) with 0.250 mL of the stock solution of Bu₄NX in Teflon-capped (1 mm) cuvettes equipped with a sidearm (solution A). Separately, 5.0 mL of the stock solution of **1** was mixed with 5.0 mL of a 0.50 M-solution of Bu₄NPF₆ in acetonitrile (solution B with the same concentration of **1** and ionic strength as solution A). After measuring the UV-Vis spectrum of solution A, x ml portions of the diluted solution B (where x = 0.125, 0.150, 0.200, 0.250, 0.300, 0.400, 0.500, 0.600, 0.750, 0.900, 1.000, 1.500, 2.000 or similar number) were added progressively and the spectra were measured after each addition. Since the concentration of **1** and the ionic strength of solution B are the same as solution A, an addition of B to A decreased concentration of iodide in the mixture, but kept the concentration of **1** and the ionic strength constant. Thus, regardless of the method of preparation of the solutions for the UV-Vis measurements, the concentrations of **1** and the ionic strength were kept constant, and the concentrations of Bu₄NX varied in a series of measurements; and the values of

formation constants derived from both types of the UV-Vis experiments were the same within the accuracy limit, except for the studies of interaction of **1** with Cl^- . Since slow side reactions were observed in the solutions containing mixtures of **1** and Cl^- , UV-Vis measurements of the interaction of Cl^- with **1** were done only using the first method, i.e. each measurement was done immediately after mixing of the reactants.

Formation constants of complexes [**1**, X^-], K in Table 1 were established via regression analysis of the UV-Vis data. An addition of X^- anions to the solutions of **1** leads to the formation of XB complexes



The formation constant of the complex, K , is expressed as

$$K = C_{\text{com}} / ((C_1^0 - C_{\text{com}})(C_X^0 - C_{\text{com}})) \quad (\text{S2})$$

where C_{com} , C_1^0 and C_X^0 are equilibrium concentration of complex and initial concentrations of **1** and halide in the mixture. Solving equation S2 leads to expression for concentration of complex as:

$$C_{\text{com}} = \{(C_1^0 + C_X^0 + 1/K) - ((C_1^0 + C_X^0 + 1/K)^2 - 4C_1^0 C_X^0)^{0.5}\} / 2 \quad (\text{S3})$$

The changes of absorption intensity at a certain wavelength upon formation of complex are

$$\Delta\text{Abs} = (\varepsilon_{\text{com}} \times C_{\text{com}} + \varepsilon_1 \times (C_1^0 - C_{\text{com}}) + \varepsilon_X \times (C_X^0 - C_{\text{com}})) - (\varepsilon_1 \times C_1^0 + \varepsilon_X \times C_X^0) l \quad (\text{S4})$$

where ε_{com} , ε_1 , and ε_X are extinction coefficients of complex, **1** and X^- at this wavelength and l is length of the UV-Vis cuvette. Since the extinction coefficients of the halide salts (and their absorption) were negligible in the spectral range which was used in the analysis, ΔAbs can be expressed as:

$$\Delta\text{Abs} = \Delta\varepsilon l \times C_{\text{com}} \quad (\text{S5})$$

where $\Delta\varepsilon$ is a difference in extinction coefficients of complex and **1**. Thus, values of ΔAbs measured in a series of solutions with the same concentration of **1** and variable concentration of X^- can be expressed as:

$$\Delta\text{Abs} = \Delta\varepsilon l \times C_{\text{com}} = \varepsilon l \times \{(C_1^0 + C_X^0 + 1/K) - ((C_1^0 + C_X^0 + 1/K)^2 - 4C_1^0 C_X^0)^{0.5}\} / 2 \quad (\text{S6})$$

Fittings of the results of the UV-Vis titrations to eq. S6 was done using Origin Pro 2016 (with ΔAbs and C_X^0 as dependent and independent variables y and x , respectively, C_1^0 as a constant and $\Delta\varepsilon$ and K as adjustable parameters). Such fittings (illustrated in Figures S1-S4) produced values of K and $\Delta\varepsilon$ in Table 1.

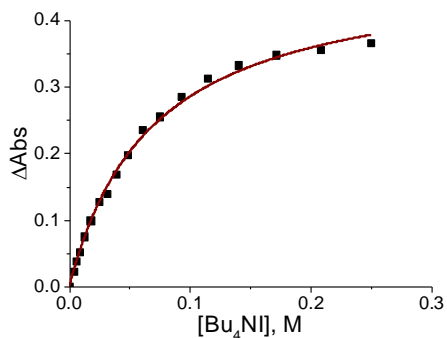


Figure S1. Dependence of differential absorbance ΔAbs (obtained by subtraction of absorption of components from the absorption of the mixture) on the concentration of Bu_4I in the acetonitrile solutions containing 0.8 mM of **1** and Bu_4NI (ionic strength was kept constant with Bu_4NPF_6).

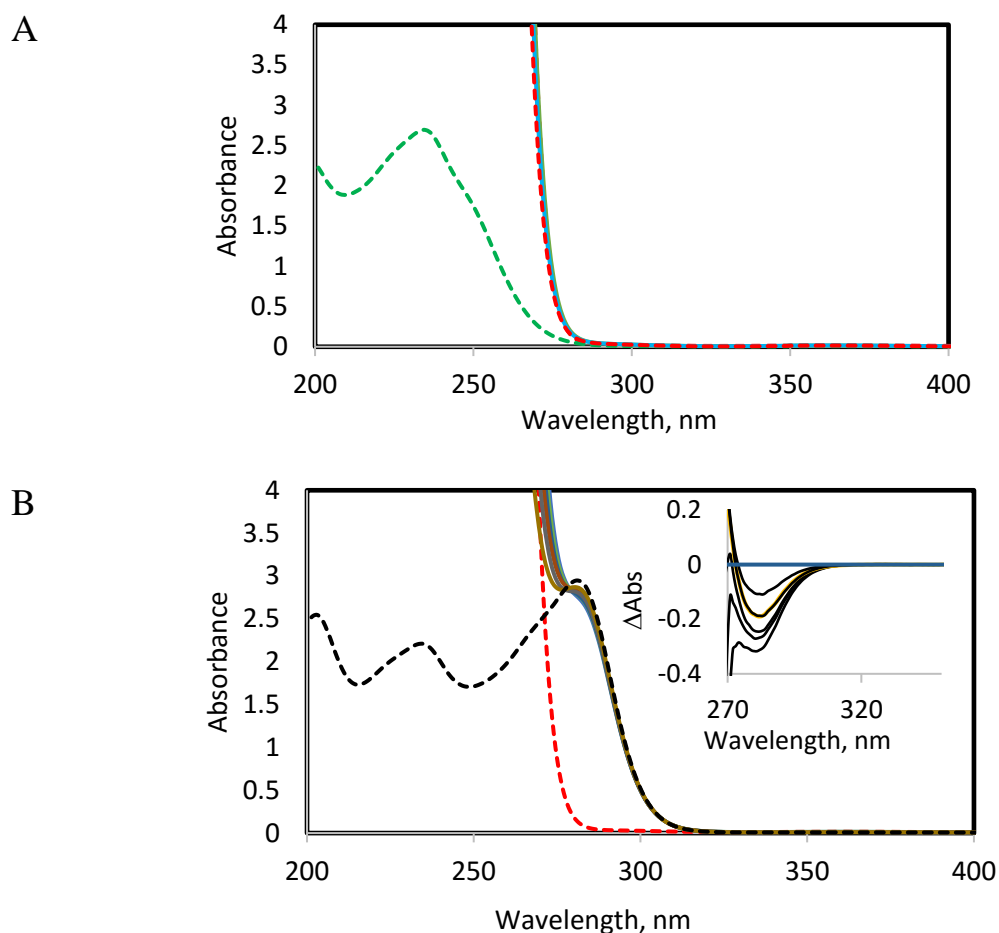


Figure S2. (A) Spectra of acetonitrile solutions of 1.5 mM **TDACl** (green dashed line), 250 mM Bu_4NI (red dashed line) and their mixtures (solid line) with the same concentrations of components. (B) Spectra of acetonitrile solutions with constant concentration of **2TDA** (2.0 mM) and various concentrations of Bu_4NI (from 0 to 250 mM). Dashed lines show spectra of the individual solutions of 2.0 mM **2TDA** (black) and of 250 mM Bu_4NI (red). Ionic strength was maintained with Bu_4NPF_6 . Insert: Differential spectra of the solutions obtained by subtraction of the absorption of components from the spectra of their mixtures.

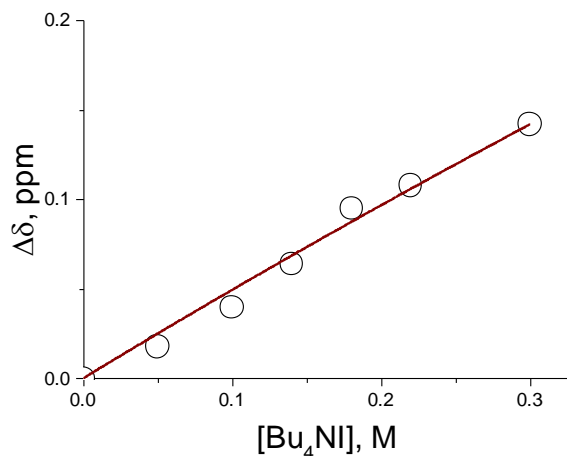


Figure S3. Dependence NMR shifts of the protons of **2** on the concentration of I⁻ anions in the solutions with constant initial concentration of **2** of 11 mM (as compared to the chemical shift of the individual **2**, in CD₃CN, 22°C, ionic strength was maintained with Bu₄NPF₆) Solid line represent a fit of the data to the expression $\Delta\delta = \Delta\delta_{\infty} C_{\text{com}} / C_2 = (\Delta\delta_{\infty} / C_2) \times \{ (C_2 + C_X + 1/K) - ((C_2 + C_X + 1/K)^2 - 4C_2 C_X)^{0.5} \} / 2$, where C_{com} is an equilibrium concentration of complex in solution, C_2 and C_X are initial concentrations of **2** and halide in the mixture, and $\Delta\delta_{\infty}$ is a limiting shift (when all **2** are hydrogen-bonded with iodide). This fitting produced value of $K = 0.22$. Note that the dependence of $\Delta\delta$ on $[\text{Bu}_4\text{NI}]$ is almost linear (since only a very small fraction of **2** are hydrogen bonded with iodides in the accessible concentration range of Bu₄NI). Therefore the value of $\Delta\delta_{\infty} = 2.23$ ppm were taken from the calculated chemical shifts of the protons of **2** (8.11 ppm) and its hydrogen-bonded complex with iodide [2, I⁻] (10.34 ppm) (GIAO ¹H NMR calculations at the M062X/def2trzvpp level in CH₃CN as a medium). \

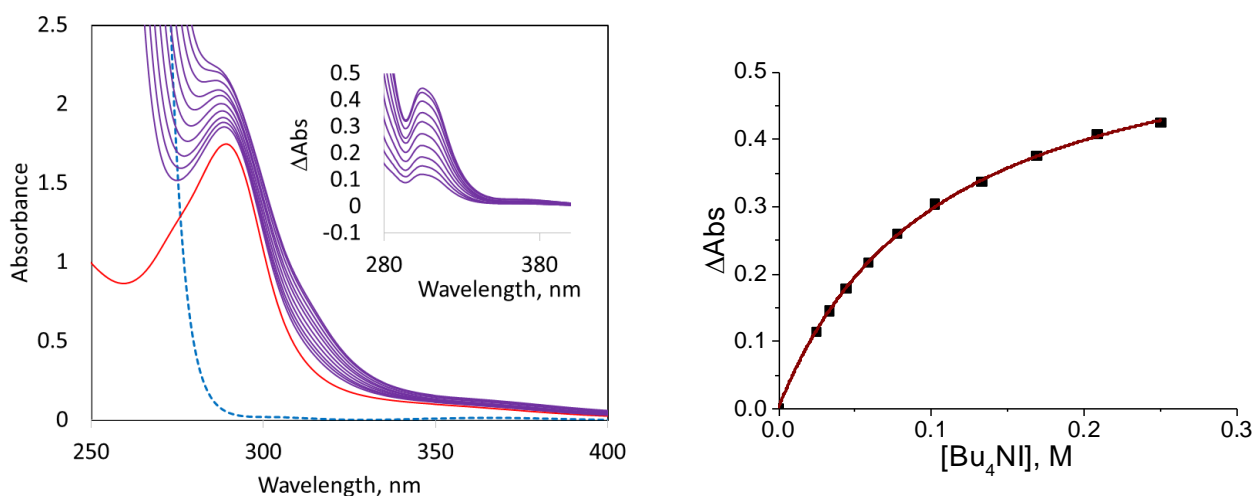


Figure S4. Left: Spectra of dichloromethane solutions with constant concentration of **1** (0.85 mM) and various concentrations of Bu₄NI (solid lines from the bottom to the top). Dashed lines show spectra of the individual solutions of 0.80 mM **1** (red) and of 250 mM Bu₄NI (blue). Ionic strength was maintained with Bu₄NPF₆. Inset: Differential spectra of the solutions obtained by subtraction of the absorption of components from the spectra of their mixtures. (Right) Dependence of differential absorbance ΔAbs (obtained by subtraction of absorption of components from the absorption of the mixture) on the concentration of Bu₄NI in these solutions.

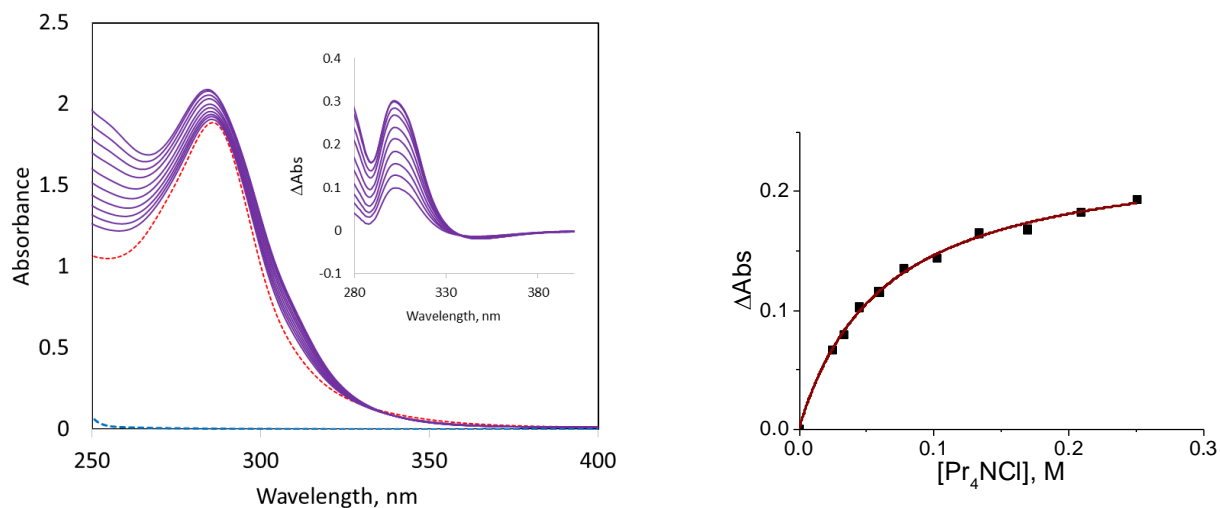


Figure S5. Left: Spectra of acetonitrile solutions with constant concentration of **1** (0.80 mM) and various concentrations of Bu₄NBr (solid lines from the bottom to the top). Dashed lines show spectra of the individual solutions of 0.80 mM **1** (red) and of 250 mM Bu₄NBr (blue). Ionic strength was maintained with Bu₄NPF₆. Inset: Differential spectra of the solutions obtained by subtraction of the absorption of components from the spectra of their mixtures. Right: Dependence of differential absorbance ΔAbs (obtained by subtraction of absorption of components from the absorption of the mixture) on the concentration of Bu₄NBr in these solutions containing.

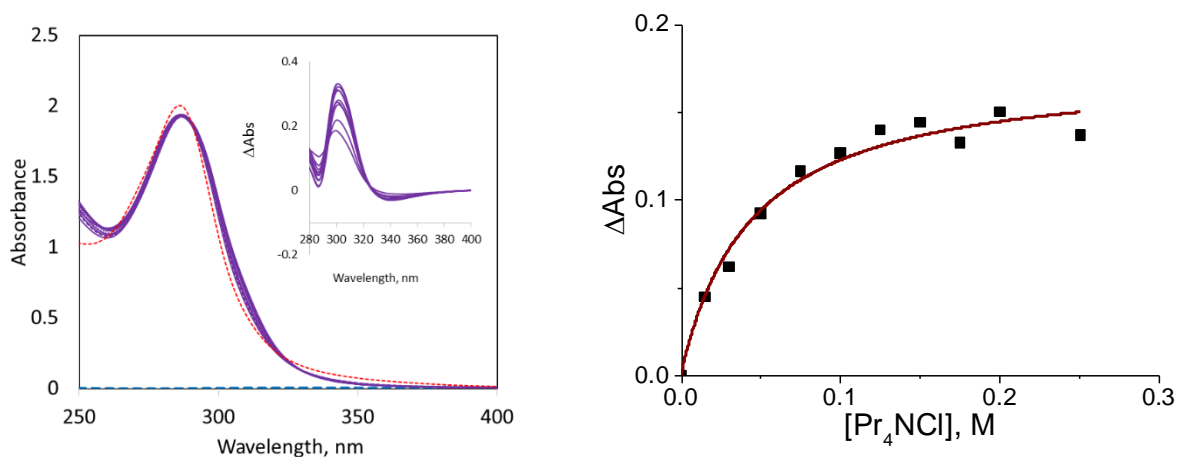


Figure S6. Left: Spectra of acetonitrile solutions with constant concentration of **1** (0.80 mM) and various concentrations of Pr₄NCl (solid lines from the bottom to the top). Dashed lines show spectra of the individual solutions of 0.80 mM **1** (red) and of 250 mM Pr₄NCl (blue). Ionic strength was maintained with Pr₄NPF₆. Inset: Differential spectra of the solutions obtained by subtraction of the absorption of components from the spectra of their mixtures. Right: Dependence of differential absorbance ΔAbs (obtained by subtraction of absorption of components from the absorption of the mixture) on the concentration of Pr₄NCl in these solutions.

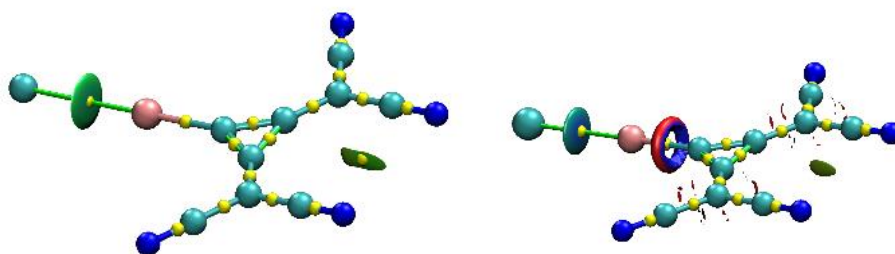


Figure S7. Optimized geometries of the $[1, \text{Br}^-]$ (left) and $[1, \text{Cl}^-]$ complexes with (3, -1) critical points (yellow spheres) and bond paths (green line) from AIM analysis and the blue-green disc indicating intermolecular attractive interactions resulting from the NCI treatments ($s = 0.4$ au isosurfaces, a color scale of -0.035 (blue) $< \rho < 0.02$ (red) au).

Table S1. Characteristics of the (3,-1) bond critical points along $\text{I} \cdots \text{X}^-$ halogen bonds (in a.u.)

Complex	ρ (density)	H(Energy density)	$\nabla^2 \rho$ (Laplacian of electron density)
$[1, \text{I}^-]$	1.49E-02	4.68E-04	3.46E-02
$[1, \text{Br}^-]$	1.79E-02	4.53E-04	4.60E-02
$[1, \text{Cl}^-]$	2.21E-02	4.37E-04	6.15E-02

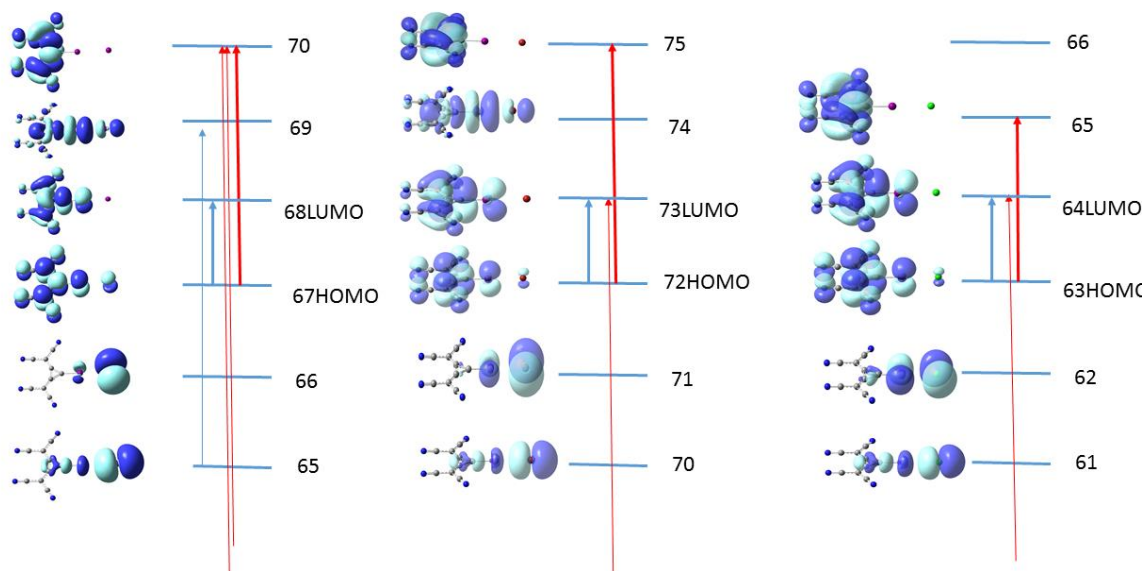


Figure S8. MO shapes and energies for $[1, \text{I}^-]$ (left), $[1, \text{Br}^-]$ (center) and $[1, \text{Cl}^-]$ (right). Blue and red arrows represent components of the transitions responsible for the appearance of the lowest-energy absorption bands in the complexes (see details from the output files of TD DFT computations below, note that oscillator strengths of excited state **1** in each case are essentially negligible, and they are not shown).

Excitation energies and oscillator strengths calculated for [1, I⁻]:

Excited State 1: Singlet-A 4.7537 eV 260.82 nm f=0.0051 <S**2>=0.000

61 -> 69 0.17095

67 -> 69 0.66012

67 -> 71 0.10259

Excited State 2: Singlet-A 4.8580 eV 255.22 nm f=0.6738 <S**2>=0.000

65 -> 69 -0.15352

67 -> 68 0.67137

Excited State 3: Singlet-A 4.9441 eV 250.77 nm f=0.7223 <S**2>=0.000

63 -> 68 -0.11512

64 -> 70 0.11454

67 -> 70 0.67911

Excitation energies and oscillator strengths calculated for [1, Br⁻]:

Excited State 1: Singlet-A 4.8664 eV 254.77 nm f=0.0075 <S**2>=0.000

66 -> 74 0.13754

68 -> 77 0.14542

72 -> 74 0.58566

72 -> 76 0.30052

Excited State 2: Singlet-A 4.8866 eV 253.72 nm f=0.5213 <S**2>=0.000

72 -> 73 0.69240

Excited State 3: Singlet-A 4.9458 eV 250.69 nm f=0.7170 <S**2>=0.000

68 -> 73 -0.11416

72 -> 75 0.68518

Excitation energies and oscillator strengths for [1, Cl⁻]:

Excited State 1: Singlet-A 4.9035 eV 252.85 nm f=0.0210 <S**2>=0.000

59 -> 68 -0.26929

63 -> 64 -0.11527

63 -> 66 0.29147

63 -> 67 0.53349

Excited State 2: Singlet-A 4.9066 eV 252.69 nm f=0.4459 <S**2>=0.000

63 -> 64 0.68575

Excited State 3: Singlet-A 4.9479 eV 250.58 nm f=0.7169 <S**2>=0.000

59 -> 64 -0.11330

63 -> 65 0.68017

Table S2. Energies and HOMO/LUMO energies of the complexes and individual reactants (M06-2X/def2tzvpp calculations, PCM model)

	Solvent	E, Hartree	E+ZPE, Hartree	E(HOMO), eV	E(LUMO), eV
[1, I ⁻]	CH ₃ CN	-1157.451835	-1157.387045	-0.25026	0.00922
[1, Br ⁻]	CH ₃ CN	-3434.011928	-3433.946936	-0.24975	0.01048
[1, Cl ⁻]	CH ₃ CN	-1320.007332	-1319.942294	-0.24873	0.01217
[1, I ⁻]	CH ₂ Cl ₂	-1157.433215	-1157.368343	-0.23414	0.02483
1	CH ₃ CN	-859.6273823	-859.562732	-0.25604	-0.00746
I ⁻	CH ₃ CN	-297.818415	-297.818415	-0.26435	0.21877
Br ⁻	CH ₃ CN	-2574.37678	-2574.37678	-0.27940	0.31332
Cl ⁻	CH ₃ CN	-460.370291	-460.370291	-0.28893	0.43374
I ⁻	CH ₂ Cl ₂	-297.810083	-297.810083	-0.24750	0.23449

Table S3. Calculated characteristics of the hypothetical anion- π [**1**, X⁻] complexes.^a

Complex	ΔE , kJ mol ⁻¹	λ_{\max} , nm	$10^{-4}\epsilon$, M ⁻¹ cm ⁻¹
1 ·I ⁻	0.7	252	3.76
1 ·Br ⁻	4.6	252	3.46
1 ·Cl ⁻	6.9	251	3.80

a) From M06-2X/def2tzvpp calculations, In CH₃CN, PCM model.

Atomic coordinates of the optimized AEXB complexes

[1, I⁻] CH₃CN				[1, Br⁻] CH₃CN			
I	0.74561200	-0.04678700	-0.01608500	I	1.25029400	-0.00020500	-0.00001400
N	-1.77282400	4.10762300	-0.00658700	N	-1.37232600	4.11671800	-0.02427500
C	-1.30316400	-0.01995800	-0.01162700	C	-0.80107500	-0.00017200	-0.00000300
N	-5.68510000	2.04487600	0.02168800	N	-5.23235800	1.95630000	0.04622300
C	-2.48905700	-0.69742000	-0.00384000	C	-1.97189400	-0.70396400	0.00017400
C	-2.38275200	3.12932000	-0.00292200	C	-1.95792500	3.12363400	-0.01190200
C	-3.12129500	1.92169900	0.00144000	C	-2.66638900	1.89839300	0.00115100
N	-5.78229600	-1.85968500	0.01984900	N	-5.23287700	-1.95519300	-0.04618800
C	-2.45625900	0.71128200	-0.00407200	C	-1.97173900	0.70388500	-0.00015600
N	-1.98151800	-4.12524600	-0.00401800	N	-1.37308200	-4.11676400	0.02422400
C	-4.53377700	1.98535600	0.01237800	C	-4.07990700	1.92697300	0.02396600
C	-3.21506300	-1.87256300	0.00202500	C	-2.66687900	-1.89829000	-0.00114600
C	-2.54019600	-3.11680200	-0.00126800	C	-1.95879200	-3.12374500	0.01189500
C	-4.62932000	-1.86217900	0.01176900	C	-4.08040900	-1.92644300	-0.02393300
I	4.28415200	0.00442100	0.01156000	Br	4.54682800	0.00005100	0.00001700
[1, I⁻] CH₂Cl₂				[1, Cl⁻] CH₃CN			
I	-0.75284700	-0.07080700	0.04252100	I	1.81581100	-0.06615900	0.00073900
N	1.72847800	4.10777500	0.01823500	N	-0.74975400	4.10492700	0.01712400
C	1.29824800	-0.03179400	0.03164900	C	-0.23997900	-0.02303700	0.00163500
N	5.65467500	2.09642100	-0.05634500	N	-4.64064000	2.00224700	-0.03381900
C	2.49297600	-0.69483100	0.01078700	C	-1.42373100	-0.70626700	0.00145800
C	2.34314800	3.13246400	0.00850400	C	-1.34957100	3.12018800	0.00860700
C	3.09339000	1.93163800	-0.00292600	C	-2.07588000	1.90574100	-0.00034600
N	5.80492900	-1.80665600	-0.05564300	N	-4.70361800	-1.91179700	0.03327600
C	2.44303600	0.71321800	0.01167500	C	-1.40001300	0.69963400	0.00125000
N	2.05285600	-4.13716100	0.01117500	N	-0.87347300	-4.12680700	-0.01438400
C	4.50492300	2.01510500	-0.03202400	C	-3.48857100	1.95571100	-0.01726900
C	3.23800000	-1.85829900	-0.00542200	C	-2.13683300	-1.89083000	0.00251900
C	2.58745700	-3.11573100	0.00330000	C	-1.44595900	-3.12592700	-0.00613200
C	4.65225900	-1.82484000	-0.03248700	C	-3.55058800	-1.89919300	0.01805700
I	-4.27747700	0.00619900	-0.03082800	Cl	4.89393300	-0.16076300	-0.00330100